FEBS Letters 581 (2007) 1027–1034

In vitro synthesis, tetramerization and single channel characterization of virus-encoded potassium channel Kcv

Ji Wook Shim[a], Mingming Yang[b], Li-Qun Gu[a,*]

[a] Department of Biological Engineering, Dalton Cardiovascular Research Center, University of Missouri, Columbia, MO 65211, USA
[b] Department of Biomedical Engineering, Duke University, Durham NC 27708, USA

Received 5 January 2007; revised 2 February 2007; accepted 2 February 2007

Available online 12 February 2007

Edited by Maurice Montal

Abstract **Chlorella virus-encoded membrane protein Kcv represents a new class of potassium channel. This 94-amino acids miniature K^+ channel consists of two *trans*-membrane α-helix domains intermediated by a pore domain that contains a highly conserved K^+ selectivity filter. Therefore, as an archetypal K^+ channel, the study of Kcv may yield valuable insights into the structure–function relationships underlying this important class of ion channel. Here, we report a series of new properties of Kcv. We first verified Kcv can be synthesized in vitro. By co-synthesis and assembly of wild-type and the tagged version of Kcv, we were able to demonstrate a tetrameric stoichiometry, a molecular structure adopted by all known K^+ channels. Most notably, the tetrameric Kcv complex retains its functional integrity in SDS (strong detergent)-containing solutions, a useful feature that allows for direct purification of protein from polyacrylamide gel. Once purified, the tetramer can form single potassium-selective ion channels in a lipid bilayer with functions consistent to the heterologously expressed Kcv. These finding suggest that the synthetic Kcv can serve as a model of virus-encoded K^+ channels; and its newly identified properties can be applied to the future study on structure-determined mechanisms such as K^+ channel functional stoichiometry.**

Keywords: Cell-free protein synthesis; Ion selectivity; Kcv; Lipid bilayer; Potassium channel; Single channel

1. Introduction

Kcv is a *Paramecium bursaria* chlorella virus (PBCV-1)-encoded membrane protein that features the essential structure of the K^+ channels from prokaryotes and eukaryotes [1–3]. When expressed in *Xenopus* oocytes [1,3], mammalian HEK293 [4] cells and Chinese hamster ovary (CHO) cells [2], Kcv yields robust K^+ selective currents sensitive to block by Ba^{2+} and amantadine [1]. This virus-encoded K^+ channel is supposed to be present in the internal membrane of the viral particle. Upon fusion of the viral membrane with the host plasma membrane, it may depolarize the local plasma membrane, promoting the viral genome release into the host [5,6]. The Kcv activities may also be regulated by phosphorylation or dephosphorylation [7]. In addition, Kcv may also participate in other important functionalities. For example, it may thermodynamically couple with virus-encoded aqua-glyceroporin to simultaneously alter water conductance and driving force for water movement [8].

While the physiological roles of Kcv are being intensively investigated [4–6,8], its unique structure is becoming a new focus. Constituted by only 94-amino acids, this miniature Kcv is the shortest K^+ channel protein ever found. It possesses the most primitive structure of all K^+ channels: two *trans*-membrane α-helix domains intermediated by a pore domain with 61% similarity and 38% identity relative to the pore regions of many other K^+ channel proteins [1]. Most notably, the pore domain of Kcv is highly conserved at the K^+ selectivity filter sequence, TXXTXGFG, which is common to virtually all K^+ channels [1]. Recently, the site-directed mutagenesis in combination with electrophysiology study based on macroscopic current recordings of heterologously expressed protein has produced a wealth of information on channel structure-related properties of Kcv. For example, Kcv is a moderate voltage-dependent, inward rectifying channel with distinct kinetics features [9]; the short N-terminus of Kcv is a possible region that modulates channel conductance [4]; and the proline kink of TM1 at the membrane/aqueous interface may control the orientation of TM1 in the lipid bilayer, therefore play an important role in the time- and voltage-dependent inward rectification [10]. Moreover, novel approach using natural diversity analysis of the Kcv family encoded by chlorella viruses [3,11] has been used to identify key amino acids (at positions of 19, 54 and 66) affecting K^+ channel properties through long distance interaction [12]. In summary, these unique structural features suggest Kcv is a model channel in research on structure-determined molecular mechanisms.

In this paper, we report a series of studies which reveal newly identified properties relating to Kcv: cell-free synthesis, molecular stoichiometry, stability in strong detergent SDS and single channel characterization. Cell-free protein synthesis is a powerful protein production tool that has advantages over conventional techniques in time-efficiency, capability of synthesis with labeled amino acids (such as S35-methionine) and simplified protein purification; thus, it has been utilized to produce a broad series of membrane proteins including ion channels [13–16], neural receptors [17], ion pumps [18], drug transporters [19] and many bacterial protein pores [20–23]. In this report, we describe Kcv synthesis using coupled IVTT technique. Through co-synthesis and assembly of the wild-type Kcv and tagged variant, we were able to separate a series of homo- and hetero-oligomer by electrophoresis, and demonstrate a tetrameric Kcv stoichiometry, a common structure adopted by all known K^+ channels. Most notably, the

*Corresponding author. Fax: +1 573 884 4232.
E-mail address: gul@missouri.edu (L.-Q. Gu).

0014-5793/$32.00
doi:10.1016/j.febslet.2007.02.005

tetrameric Kcv retains its functional integrity in SDS-containing solution. With this capability, the tetramer can be directly purified from polyacrylamide gel and form single K^+ channels in the lipid bilayer.

We are motivated to study Kcv due to its potential in elucidating the K^+ channel functional stoichiometry, a structural–functional relationship that regulates how the functions of the K^+ channel such as high K^+ selectivity depend on the individual contribution by each of the four identical subunits. It is known that the four identical subunits in a K^+ channel are symmetrically associated and work concertedly in conferring unique functions on channels [24–29]. Our interest is the modulation of channel properties by each subunit individually in a tetramer [30–32]. The strategy of this investigation is to detect hetero-channels that contain different numbers of functionally-inactive subunits. According to the findings in this report, the miniature K^+ channel Kcv is suitable to this investigation, since the hetero-Kcv proteins can separate in the gel and the Kcv tetramer purified from gel can function as a K^+ channel. These properties could be very useful for detecting each hetero-Kcv channel individually. Ultimately, we are able to investigate at the single channel level the impact of such hetero-Kcv structures on the channel properties.

2. Materials and methods

2.1. Kcv gene assembly and amplification

With the aid of software DNAWorks [33], the Kcv gene was optimized for *Escherichia coli* expression from its known amino acid sequence [3], and was assembled and amplified from oligonucleotides by PCR. All the oligonucleotides were limited to 50 nucleotides in length; the annealing temperature T_m, (evaluated from the GC content) of optimized oligonucleotides was 58 °C with a range of 1.6 °C; and the total codon usage score was 0.725. Unique *Nde*I and *Hind*III cloning sites (underlined below) as well as stop codons (lower case below) were also introduced. The forward and reverse strands were each assembled from seven overlapping oligonucleotides:

Forward strand
5′CATATGTTAGTGTTTTCTAAATTCCTGACC,
CGCACGGAACCATTTATGATCCACTTATTCATCTTAGCGA-TGTTTGT,
GATGATTTACAAGTTCTTTCCGGGTGGCTTTGAGAACAAC-TTCTCT,
GTGGCGAATCCGGCACAAAAAAGCGTCTTGGATTGATTG-TATTTATTT,
TGGTGTGACCACCCACTCTACCGTTGGTTTCGGTGATAT,
CTTACCAAAAACGACGGGCGCGAAACTGTGCACGATC
GCCCACATTGTGACGGTGTTCTTTATTGTTTTAACCCTG-tgataaG,
and reverse strand
5′AAGCttatcaCAGGGTTAAAACAATAAAGAAC,
ACCGTCACAATGTGGGCGATCGTGCACAGTTTCGC,
GCCCGTCGTTTTTGGTAAGATATCACCGAAACCAACGG-TAG,
AGTGGGTGGTCACACCAAAATAAATACAATCAATCCAAG-ACGCTTTT,
TTGTCCGGATTCGCCACAGAGAAGTTGTTCTCAAAGCCA,
CCCGGAAAGAACTTGTAAATCATCACAAACATCGCTAAGA-TGAATAAGTG
GATCATAAATGGTTCCGTGCGGGTCAGGAATTTAGAAAA-CACTAACATAT.

For gene assembly and amplification, PCR was carried out in a 50 μl mixture containing 25 μl of oligonucleotides and 25 μl of enzyme mix (FideliTaq; #71182, USB). The tube contained 1 pmol of each oligonucleotide except for the 5′-end oligonucleotides for each DNA strand. These two oligonucleotides also functioned as amplification primers and were present at 50-fold molar excess over the internal ones to achieve both assembly and amplification in a simple, one-tube protocol [34]. After an initial heating segment at 95 °C for 5 min, the reaction was cycled for 0.5 min at 94 °C, followed by "touch down" annealing [35] from 68 °C to 58 °C for 0.5 min (in 1° decrements per cycle) and concluding with a 0.5 min extension at 68 °C. When the lowest annealing temperature was reached, conventional PCR was continued for an additional 19 cycles under the last "touch down" parameters. The program ended with a final extension step at 68 °C for 10 min.

2.2. Incorporation of Kcv gene into plasmid

The full-length Kcv gene obtained by PCR (above) was purified on a 1% agarose–TBE gel and inserted directly into a TA vector (TOPO-TA; #K4500-01, Invitrogen). After verification by sequencing, the gene was liberated from the TA vector by digestion with *Nde*I and *Hind*III and ligated with pT7-SC6 that had been cut by the same enzymes to yield pT7-Kcv.

2.3. Modified Kcv genes

To purify Kcv and determine its subunit stoichiometry, DNA encoding an N-terminal His tag with an oligo-aspartate linker [36] was appended to the wild type gene. The amino acid sequence of the complete tag is: MHHHHHHDDDDDDDDSMG. This tag, which is present in pT7-SC7, lies between unique *Nde*I and *Nco*I sites (underlined) and contains the following sequence: 5′CATATG CACCAT-CACCACCATCATAATAACAATAATAACAACAATAATTCCA-TGGC. Once insertion of this N-terminal sequence onto the Kcv gene was achieved through PCR, homologous recombination of the resulting fragments was performed [37]. One of these fragments was generated using *Eco*NI-linearized pT7-SC7 as a template with (forward) 5′GACGACGATGATTCCATGGGCTTAGTGTTTTCTAAATTC-CTG and (reverse) 5′CAGAAGTGGTCCTGCAACTTTAT as primers. The other fragment used for homologous recombination was derived from *Hind*III-linearized pT7-Kcv using PCR with primers (forward) 5′ATAAAGTTGCAGGACCACTTCTG and (reverse) 5′ATAAAGTTGCAGGACCACTTCTG. The resulting tagged Kcv gene in the T7 expression vector (pT7-H6D8-Kcv) was used to generate hetero-oligomers with the wild type gene.

Later, however, expression work using *E. coli* S30 extracts showed that this tag was rapidly proteolysed, possibly inferring that acid proteases in the extract were acting on the aspartate motif. To prevent proteolysis, the aspartic acid residues of the tag were replaced with asparagines. This strategy proved successful as little or no proteolysis was observed in S30 extracts when Kcv carried a polyasparagine linker at its N-terminus. To introduce a His tag and octo-asparagine linker on Kcv, pT7-D8H6-Kcv (see above) was digested with *Nde*I and *Nco*I, and the resulting small fragment was replaced with two oligonucleotide cassettes that encode the new tag to yield pT7-H6N8-Kcv, cassette 1: 5′TATGCACCATCACCACCATCATAAT (sense), phosphorylated 5′GTTATTATGATGGTGGTGATGGTGCA (antisense); and cassette 2: 5′phosphorylated AACAATAATAACAACAATAATTC (sense), 5′CATGGAATTATTGTTGTTATTATT (antisense). All modified genes were subsequently verified by DNA sequencing.

2.4. In vitro transcription and translation

In vitro radiolabeled wild type and tagged Kcv polypeptides were synthesized by coupled IVTT in the presence of [^{35}S] methionine (10 μCi per 25 μl reaction, 1200 Ci/mmol, ICN) and rifampicin (20 μg/ml), with an *E. coli* T7 S30 extract (Promega) as previously described [21]. The DNA template (4 μl, 40 ng/μl) was incubated with IVTT components containing complete amino acid mix for 1 h at 37 °C, with a yield of about 200 ng/ml by comparison with the in vitro-synthetic α-hemolysin in earlier reports [20,21].

2.5. Hetero-tetramer formation

Early work had shown that the wild type Kcv polypeptide spontaneously assembles into an SDS-stabile oligomer during in vitro synthesis. To determine the stoichiometry of this oligomer, wild type and tagged Kcv proteins were co-synthesized and assembled in vitro, as described above, with various DNA ratios (4:0, 3:1 2:2, 1:3 and 0:4) of pT7-Kcv and pT7-H6N8-Kcv, respectively. The resulting homo- and hetero-oligomers were loaded on a 12.5% SDS–polyacrylamide gel [38] and electrophoresed. The gel was then dried and exposed to X-ray film.

2.6. Purification of the Kcv oligomer for planar bilayer recordings

For bilayer recordings, wild type Kcv was synthesized as above, except for the inclusion of rabbit red blood cell membranes (10 μl; 1 mg/ml protein) during IVTT, as previously described [21]. After IVTT, membranes were spun down (5 min at 21 000 × *g*) and washed with 500 μl of MBSA buffer (10 mM Na MOPS, titrated with NaOH, 150 mM NaCl, 0.1% BSA; pH 7.0). The washed membranes were repelleted and then solubilized in 50 μl of sample buffer prior to electrophoresis on a 12% SDS–polyacrylamide gel [38]. Immediately after electrophoresis, the gel was dried between two sheets of plastic film (#V713B; Promega) using an air-drying system (''GelAir'', #165-1771, Bio-Rad) at 50 °C for 2 h, and exposed to X-ray film. Using the developed autoradiogram as a template, a slice containing the Kcv oligomer was excised from the gel with scissors and rehydrated in a tube with 0.5 ml of water. After rehydration, the plastic film backings were released from the gel slice and subsequently removed with flamed metal forceps. The slice was then crushed in the tube with a disposable plastic pestle (#749521-1590; Nalge Nunc International) and the resulting gel fragments were removed with a spin filter (''QIAshredder'', #79654; Qiagen). The filtrate containing the Kcv oligomer was stored frozen in 50 μl aliquots at −80 °C.

2.7. Single channel recording on planar lipid bilayer system

The planar lipid bilayer apparatus is composed of a 25-μm-thick Teflon film (Goodfellow, Malvern, MA) with a 100-μm diameter orifice serving as the partition between the two 2-ml Teflon chambers (made by Science Workshop at University of Missouri). The orifice was pretreated with 1:10 hexadecane (J.T. Baker)/pentane (Burdick and Jackson). A solvent free planar lipid bilayer of 1,2-diphytanoyl-*sn*-glycerophosphatidylcholine (Avanti Polar Lipids) was formed over the orifice by a mono-layer folding method [39]; a potential was applied across this bilayer by Ag/AgCl electrodes with 1.5% agarose (Ultra Pure DNA Grade, Bio-Rad) bridges containing 3 M KCl. Protein was added to the *cis* chamber, which was grounded, while voltage was applied from the *trans* chamber so that at positive potential a positive current was recorded, representing cations flowing from *trans* to *cis*. Single-channel currents were recorded with an Axopatch 200B patch-clamp amplifier (Molecular Device Inc.), filtered at 1 kHz with a built-in 4-pole low-pass Bessel Filter, and acquired with Clampex 9.0 software (Molecular Device Inc.) through a Digidata 1332 A/D converter (Molecular Device Inc.) at a sampling rate of 20 kHz. The current noise I_{RMS} is 1.2–1.5 pA (the value of I_{RMS} displayed on the amplifier panel). The Data were analyzed using Clampex 9.0, Excel 2003 (MicroSoft) and SigmaPlot (SPSS) software. All the single channel currents were determined by fitting the peaks in amplitude histograms to Gaussian functions. Conductance values were given as means ± S.D. based on n separate experiments ($n \geqslant 3$). The electrophysiology experiments were conducted at 22 ± 2 °C.

3. Results

3.1. In vitro synthesis and oligomerization of Kcv

The S35-labeled membrane protein Kcv was synthesized by coupled IVTT as described in Section 2. The protein product can be detected by electrophoresis on the SDS–polyacrylamide gel (Fig. 1). The synthetic wild type (wt-) Kcv generates two major bands in the 12.5% SDS gel (Lane-A): a light band below 14-kDa, and a heavy band above 32 kDa. Considering the molecular weight of Kcv (10.6 kDa) [1], we associate the light species to protein in monomeric format—suggesting the successful synthesis of Kcv, and the heavy species to the product of Kcv monomer oligomerization. There are several indicators that support this explanation. First, only S35-labeled protein

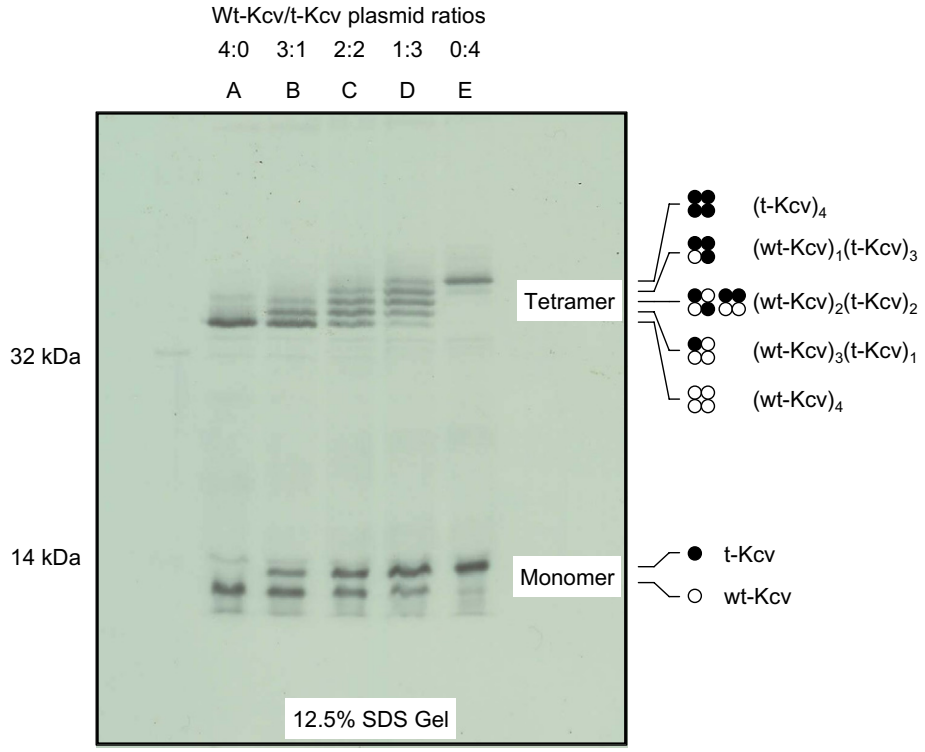

Fig. 1. Electrophoretically separated monomers, homo- and hetero-tetramers of in vitro-synthesized Kcv. All S35-labeled proteins were produced from coupled IVTT, run on a 12.5% SDS–polyacryamide gel, and visualized by autoradiograph. Lane-A: wild type Kcv (wt-Kcv); Lanes-B–D: cosynthesized wt-Kcv and tagged Kcv (t-Kcv) at wt-Kcv:t-Kcv DNA ratios of 1:3, 2:2 and 3:1, respectively; Lane-E: synthetic t-Kcv only. Lane-A and Lane-E each contain one light band below 14 kDa and one heavy band above 32 kDa, while Lanes-B–D each contains two light bands and five heavy bands. Light bands represent monomers of wt- and/or t-Kcv, and together the five heavy bands represent all possible combinations of homo- and hetero-tetramers co-assembled by wt-/t-Kcv.

can be resolved in the gel, which rules out the possibility of other proteins contributing to the band as the only radio-labeled protein present during in vitro-synthesis is wt-Kcv. Second, upon heating the in vitro product at 100 °C (Fig. S1 in Supplementary material) the heavy band diminishes and protein is transferred to the light band, suggesting that Kcv oligomer that dissociates into monomers at high temperature is the only component present in the heavy band. Third, no other major species were identified above or below the heavy band, implying that only one oligomeric format is adopted by Kcv.

In order to further verify the in vitro synthesis and oligomerization, we constructed tagged Kcv (t-Kcv), a mutant possessing a short peptide tag of six histidines and eight asparagines that serve as a linker appended to the N-terminal of wt-Kcv. This method relies upon the assumption that if t-Kcv can be synthesized and oligomerized, both its monomers and oligomers should migrate slower than wt-Kcv due to their higher molecular weights. And indeed we identified two bands for synthetic t-Kcv (Fig. 1, Lane-E), one light and one heavy, but both apparently heavier than their corresponding wt-Kcv bands (Fig. 1, Lane-A).

The results from these experiments confirm the following Kcv properties: first, the Kcv protein can be synthesized in vitro; second, the synthetic Kcv can be oligomerized; and third, the Kcv oligomer can separate by electrophoresis, suggesting its structural stability in detergent SDS.

3.2. Tetrameric molecular stoichiometry

While the above experiments verify Kcv oligomerization, the number of monomers that must associate to form the oligomer remains in question. To resolve subunit stoichiometry, we co-synthesized wt-Kcv/t-Kcv in vitro at various plasmid ratios (Fig. 1, Lanes-B–D). If wt-Kcv and t-Kcv can be co-assembled into homo- and hetero-oligomers, these co-assemblies are expected to separate in gel according to their molecular weights [20,30–32,40]. Similar methods have been developed to determine structural stoichiometry for α-helical channels [30,32,41] and β-barrel protein pores [20,21,42], where two forms of channel proteins, one differing from the other in the length of a terminal tag, were expressed either individually to form homo-oligomeric complexes, or co-expressed to form hetero-oligomers. In our study, since Kcv oligomers retain their structural integrity in SDS, we hope to discriminate various hetero-oligomers formed by co-synthesized wt-Kcv/t-Kcv present in a gel, then determine the molecular composition of Kcv via stoichiometry.

Our electrophoresis results revealed that the co-synthesized proteins split into two light bands and five heavy bands at all wt-Kcv/t-Kcv DNA ratios tested: 3:1 (Fig. 1, Lane-B), 2:2 (Fig. 1, Lane-C) and 1:3 (Fig. 1, Lane-D). Comparing these gels with bands at the same levels in Lane-A and Lane-E, we might associate the two light bands to wt-Kcv and t-Kcv monomers, respectively. This association agrees with the relative protein quantities found in each band at different DNA percentages. For example, faster-migrating wt-Kcv monomers dominate in the two lighter bands when its DNA percentage is twofold higher than t-Kcv (Lane-B); alternatively, slower-migrating t-Kcv monomers dominate when the DNA ratio is inverted (Lane-D).

Compared with the light bands, the co-synthesized products split into five heavy bands. In addition to the fastest and the slowest migrating products, which correspond to homo-oligomeric wt-Kcv and t-Kcv, three novel intermediate bands appear. The relative protein amounts in the five bands are also highly influenced by the DNA ratio. When the quantity of wt-Kcv DNA is twofold more than that of t-Kcv DNA, the faster-migrating bands dominate (Lane-B); as the quantity of wt-Kcv DNA equals that of t-Kcv DNA, the intermediate bands thicken (Lane-C); and when wt-Kcv DNA falls to one third of t-Kcv DNA, the slower-migrating bands dominate (Lane-D), an inverse trend to Lane-B. The presence of the five bands at all the tested DNA ratios not only confirms the existence of wt-Kcv/t-Kcv co-assemblies with each monomer serving as a randomly associating subunit, but also shows that there are exactly four subunits in each oligomer. Given this tetrameric stoichiometry, we can infer that the five heavy bands represent all possible combinations of wt-Kcv/t-Kcv homo- and hetero-tetramers, listed here from the fastestmigrating to the slowest-migrating species: $(\text{wt-Kcv})_4$, $(\text{wt-Kcv})_3$ $(\text{t-Kcv})_1$, $(\text{wt-Kcv})_2$ $(\text{t-Kcv})_2$, $(\text{wt-Kcv})_1$ $(\text{t-Kcv})_3$, and $(\text{t-Kcv})_4$, where the subscripts denote the contributed numbers of each subunit to the tetramer. In addition, the tetrameric stoichiometry is also consistent with the position of heavy bands above 32 kDa of the marker, as the presumed molecular weight of a Kcv tetramer is 42 kDa.

In summary, co-synthesizing wild-type Kcv and tagged-variant in the above experiment helps to resolve the tetrameric stoichiometry of Kcv, a universal structure adopted by all the K^+ channels. It should be noted the synthetic Kcv is tetramerized in a membrane-free system; thus it is not the membrane that promotes the protein assembling. To confirm this note, we further tested the effect of rabbit blood cell (RBC) membrane on the Kcv oligomerization (Fig. S1 in Supplementary material). It is known that many transmembrane protein pores secreted by bacteria can be oligomerized in the presence of RBC membrane [20–23]. However, our test indicated RBC membrane does not enhance the Kcv oligomer formation (Fig. S1 in Supplementary material). Since the Kcv oligomers are observed on SDS containing gel, future tests need to be done to identify the detergent effect on the Kcv oligomerization. Detergents have been reported to be compatible with and to promote the cell-free synthesis of α-helical-structured channel proteins, such as the large mechanosensitive ion channel (MscL) [14], in the absence of membrane.

3.3. Formation of single K^+ channels by Kcv tetramer purified from gel

Since natural K^+ channels commonly adopt the tetrameric structure, we questioned whether synthetic Kcv tetramer is capable of functioning as a K^+ channel. To investigate this, we collected the heavy band of gel containing wt-Kcv tetramer and dissolved it in 50 μl of water. Upon removal of the gel component by filtration, we obtained the purified protein in solution (see Section 2). The protein solution was then directly added to the *cis* chamber to allow observation of channel-forming activity.

The Kcv tetramer collected from gel rapidly formed single ion channels on the DPhPC bilayer membrane (Fig. 2). On average, single channels appeared within 5–10 min after addition of 1–2 μl of protein solution. Through measuring the fully-open current in 150 mM KCl (pH 7.2) symmetrical recording solution at various voltages (Fig. 2A), we obtained

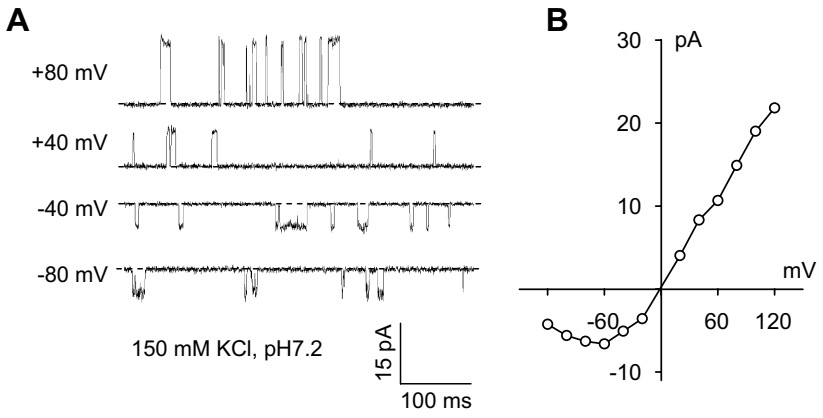

Fig. 2. Formation of ion channels by single Kcv tetramers on a DPhPC lipid bilayer. Kcv was synthesized using IVTT and self-assembled into tetrameric complex. The purified tetramer was obtained by directly collecting samples from gel and dissolving in water. The transmembrane potential for each current trace is indicated and the dashed line indicates zero current. (A) Representative current recordings from single Kcv channels at various voltages. All traces were recorded in symmetrical buffers containing 150 mM KCl and 10 mM Tris (pH 7.2). (B) Current–voltage relationship (*I–V* curve) measured from a single Kcv channel.

a Kcv current–voltage curve (*I–V* curve, Fig. 2B), which revealed a rectified *I–V* relationship: the single channel current increased almost linearly with positively applied voltages ($g = 179 \pm 21$ pS at +120 mV), but decayed sharply at negative voltages with a maximum current around −60 mV ($g = 112 \pm 11$ pS). This result is consistent with the rectified current found for Kcv channels expressed in heterologous systems [1,3].

To determine the ion selectivity of the synthetic Kcv, we first examined whether the single channel current is carried by the cations or the anions in asymmetrical KCl solutions. *I–V* data were recorded with 150 mM KCl in the *cis* chamber and 1000 mM KCl in the trans chamber (Fig. 3A and B); and the reversal potential was obtained by fitting the *I–V* data to polynomial curve. Under this asymmetrical salt condition, the reversal potential is -43.3 ± 0.3 mV, suggesting that the synthetic Kcv is very highly selective for K^+ over Cl^-. Next, we examined the Kcv channel selectivity for different cations using asymmetrical solutions containing K^+ and Na^+. *I–V* data were then recorded with 150 mM NaCl in the *cis* chamber and

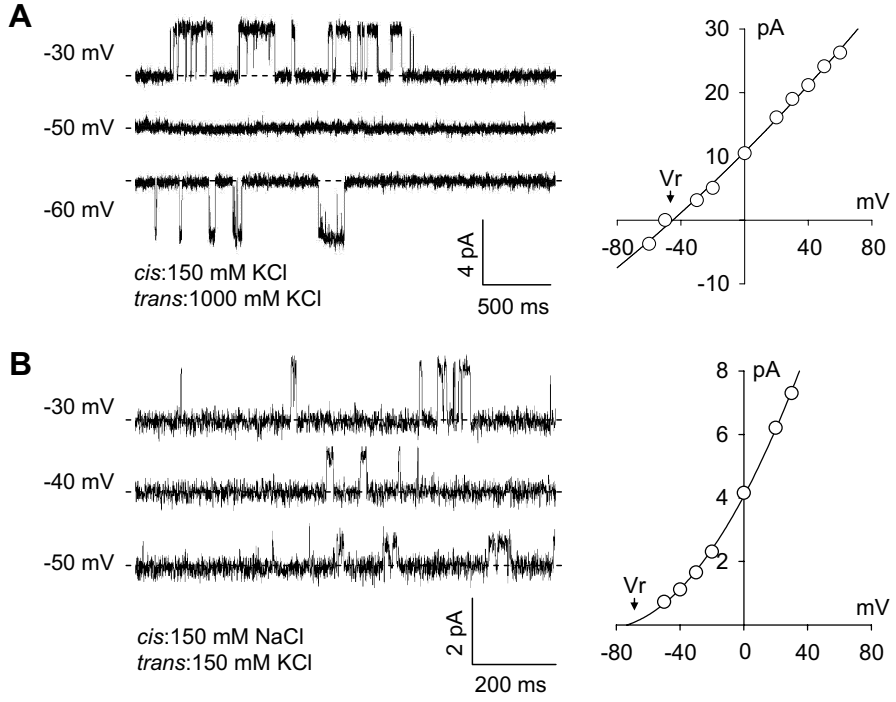

Fig. 3. Potassium selectivity of ion channels formed by Kcv tetramers. (A) Current recordings in asymmetrical KCl solutions with 150 mM KCl in the *cis* chamber and 1000 mM KCl in the *trans* chamber, and both in 10 mM Tris buffer (pH 7.2). (B) *I–V* curve recorded to test charge selectivity for Kcv based on recordings in (A). The reversal potential (V_r) is marked by the arrow. (C) Current recordings in bi-ionic asymmetrical solutions with 150 mM NaCl in *cis* and 150 mM KCl in *trans*, and both in 10 mM Tris buffer (pH 7.2). (D) *I–V* curves recorded from (C) to test cation selectivity. Again, the reversal potential (V_r) is marked by the arrow.

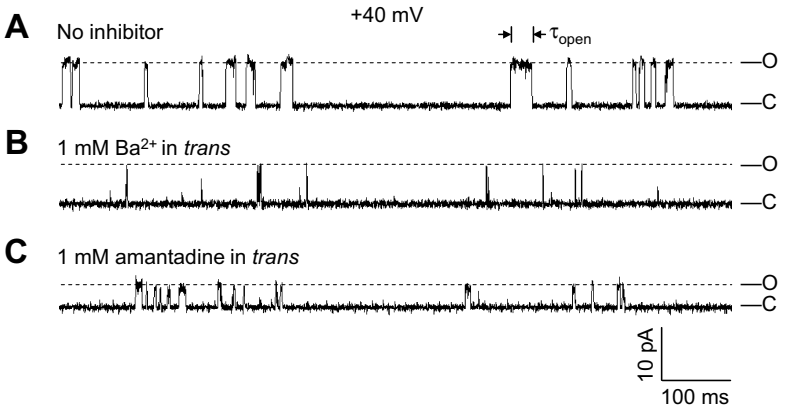

Fig. 4. Single channel current traces showing synthetic Kcv blocked by Ba^{2+} and amantadine. All solutions contained 150 mM KCl, 10 mM Tris (pH 7.2), and all the current traces shown were recorded at +40 mV. (A) Control test without any blocker at either *trans* or *cis* chamber; (B) 1 mM $BaCl_2$ presented in the *trans* side of channel, and (C) 1 mM amantadine in the *trans* chamber.

150 mM KCl in the *trans* chamber (Fig. 3C and D). Under this condition, we characterized that the channel becomes permanently closed from −50 mV, giving no current data point below this voltage; and all recorded currents are positive (Fig. 3D). In this case, the reversal potential was obtained by fitting the *I–V* data to a polynomial curve and extrapolating it to the voltage axis. The resulting reversal potential is −73.6 ± 0.4 mV, indicating that the selectivity of Kcv channel for K^+ over Na^+ is at least an order of magnitude. This result is comparable to the K^+/Na^+ permeability ratio measured for Kcv by macroscopic current recording on oocyte membrane [1].

The K^+ current recorded from Kcv channels expressed in the oocyte membrane can be inhibited by the typical K^+ channel blocker Ba^{2+} and the anti-viral drug amantadine [1]. To verify that our synthetic Kcv has the similar property, we tested the two blockers on it. The test was performed in symmetrical 150 mM KCl solutions and single Kcv channel were recorded at +40 mV. In the control test without blockers in either chamber, the typical single Kcv channel events can be identified as a series of open-close transitions (Fig. 4A) with characteristic open-state conductance (g = 207 pS), and open event duration (τ_{open} = 3.4 ms). Upon addition of 1 mM Ba^{2+} to the *trans* chamber, τ_{open} dramatically falls (τ_{open} = 0.51 ms), but g is not affected. It should be noted that many opening events in the presence of 1 mM Ba^{2+} are very short and could not be fully resolved at 1 kHz filtering frequency. As a result, it looks like that the amplitude of these events is reduced (Fig. 4B). These events were finally excluded from the conductance measurement. This result of this experiment suggests that *trans* Ba^{2+} strongly inhibits single channel open-probability through shortening open event duration and reducing its occurrence without affecting the channel conductance. We further tested the effect of amantadine on the Kcv channel current (Fig. 4C). In contrast to Ba^{2+}, we found the addition of 1 mM amantadine to the *trans* chamber does not alter τ_{open}, but instead causes 53% reduction of the channel conductance (g = 97 pS) (Fig. 4C). Thus, *trans* amantadine can also inhibit K^+ current of Kcv, but governed by a binding mechanism differing from *trans* Ba^{2+}. Similar block modes can also be observed when Barium and amantadine are presented in the *cis* chamber where protein was added (trace not shown). For example, at −40 mV, the addition of 1 mM *cis* Ba^{2+} is able to decrease the open event duration from 3.8 ms to 1.6 ms without altering the conductance, while at the same voltage, 1 mM *cis* amantadine reduces the conductance from 128 pS to 105 pS, but does not affect the open event duration. Therefore in general, it is concluded that the K^+ current of our in vitro-synthetic Kcv channel can be inhibited by either Ba^{2+} or amantadine from both sides of channel. This is in consistence with the results obtained from Kcv expressed in oocyte membrane: full current inhibition by Ba^{2+} and half inhibition by amantadine at the same inhibitor concentrations [1].

The above series of single channel characterizations suggests an important property that the Kcv tetramer retains the functional integrity in SDS. This capability allows the tetramer to be purified from the gel and to function as a K^+ channel in the artificial bilayer.

4. Discussion

In summary, here are the overall conclusions of this report: (1) the miniature virus-encoded membrane protein Kcv can be synthesized in vitro; (2) the synthetic Kcv adopts tetrameric structure and can separate by electrophoresis; (3) the Kcv tetramer retains structural and functional stability in the presence of strong detergent SDS; and (4) once purified from the gel, the Kcv tetramer is able to form single K^+-selective channels in bilayer. These findings support the following discussion.

First, cell-free protein synthesis has been shown to be an efficient protein production tool for future research applications. Second, since Kcv represents an independent class of K^+ channels encoded by virus, the confirmation of its molecular stoichiometry supports the universality of tetrameric structures among K^+ channels across all eukaryotes, prokaryotes, and now viruses [26]. Third, because functions of the synthetic Kcv are in consistence with that of the Kcv channels expressed in heterologous systems, the synthetic Kcv can be used to model the behavior of virus-encoded K^+ channels for future research on the molecular mechanisms governing channel permeation, selectivity, gating, protein–lipid interaction and pharmacology. Fourth, it is convincing that many single channel properties of our in vitro synthetic protein are identical to that of Kcv purified from yeast and inserted in artificial lipid bilayer [43], with respect to the conductance, the shape of *I–V* curve,

oligomer stability and Barium block mode. Such agreement in single channel properties between the in vitro and *in vivo* synthesized channels should implicate that the protein post-translational modification as well as the bilayer artifact can be ruled out; and the tetramerization of Kcv channel is a self-organizing process. Fifth, the Kcv tetramer remains its functional integrity after purification from SDS gel, as demonstrated by its capability to efficiently form K^+ channels in a lipid bilayer. This is notable because many β-barrel protein pores, as exemplified by α-hemolysin, also retain their oligomeric structure and pore-forming capabilities after treating with SDS [20–23]. Thus, the synthetic Kcv can also serve to model and direct the engineering of α-helical proteins that retain both structural and functional integrity under harsh biological conditions.

In addition, the single channel technique utilized in this research also exhibits its ability to reveal molecular processes. As demonstrated by the Kcv inhibition experiment (Fig. 4), single channel recordings clearly visualize distinguished inhibition mechanisms by Ba^{2+} and amantadine, as reflected by their different single molecular binding patterns (Fig. 4); this phenomenon has not been directly observed using other methods. The mechanisms for Kcv inhibition will be investigated in the future.

Regarding the planar bilayer system, it is a very efficient facility for single channel study that allows free manipulation of membrane and experimental conditions on both sides such as the lipid composition, solution pH and ion strength. Since Kcv possesses shorter transmembrane domains, particularly the C-terminal a-helical bundle, than other K^+ channels, it would be important to test how the lipid molecular length and membrane composition regulate Kcv functionalities so that the protein–lipid interaction can be modeled [2]. Recently, a modular ion channel chip based on this low noise bilayer system has been created that features both high portability and durability, with which the long-term (3 days) dynamic of Kcv channel has been observed [44].

We hope the miniature K^+ channel Kcv could serve to model the functional stoichiometry—the individual contribution by each subunits to the overall channel functionalities. In traditional methods, the wild-type protein and functionally-inactive mutant were co-expressed to form a series of homo- and hetero-oligomeric channels in the cell membrane. For single channel examination, these channel species were randomly selected in each recording without knowing their subunit composition [30–32,41]. Therefore, it was difficult to associate observed current types to each channel species. By comparison, the hetero-Kcv complexes can separate using electrophoresis, and at least the wild-type Kcv tetramer purified from the gel functions properly as a K^+ channel. Moreover, the processes already exist to separate heteromeric β-barrel protein pores [21,45–48]. We speculate that the adaptation of these processes may be capable of purifying Kcv hetero-tetramers. This would allow selectively manipulating key amino acids of an individual subunit in a protein complex. Such an exploration could be started from existing species such as the wild type Kcv and mutant F66A, a variant with a diminished K^+ current due to the substitution of Phe66 at the selectivity filter GFG [1]. It is thought that a series of relationships between the subunit compositions and the corresponding K^+ selectivity could be established; this should infer the impact of individual substitution on the overall K^+ selectivity.

Acknowledgements: We thank Stephen Cheley for the design and synthesis of the wild type and tagged Kcv genes as well as the determination of the stoichiometry of their encoded subunits while working in the laboratory of Professor Hagan Bayley at Texas A&M University. We also thank Mr. Qiulin Tan for the Kcv heating experiment and protein quantification. This investigation was supported by the University of Missouri Research Board and research council, partially supported by NSF Career Award 0546165, and conducted in a facility constructed with support from Research Facilities Improvement Program Grant C06-RR-016489-01 from the National Center for Research Resources, National Institutes of Health.

Appendix A. Supplementary data

Supplementary data associated with this article can be found, in the online version, at doi:10.1016/j.febslet.2007.02.005.

References

[1] Plugge, B. et al. (2000) A potassium channel protein encoded by chlorella virus PBCV-1. Science 287, 1641–1644.
[2] Gazzarrini, S. et al. (2003) The viral potassium channel Kcv: structural and functional features. Febs Letters 552, 12–16.
[3] Kang, M. et al. (2004) Small potassium ion channel proteins encoded by chlorella viruses. Proceedings of the National Academy of Sciences of the United States of America 101, 5318–5324.
[4] Moroni, A. et al. (2002) The short N-terminus is required for functional expression of the virus-encoded miniature K^+ channel Kcv. Febs Letters 530, 65–69.
[5] Frohns, F. et al. (2006) Potassium ion channels of chlorella viruses cause rapid depolarization of host cells during infection. Journal of Virology 80, 2437–2444.
[6] Mehmel, M. et al. (2003) Possible function for virus encoded K^+ channel Kcv in the replication of chlorella virus PBCV-1. Febs Letters 552, 7–11.
[7] Kang, M. et al. (2004) Genetic diversity in chlorella viruses flanking kcv, a gene that encodes a potassium ion channel protein. Virology 326, 150–159.
[8] Gazzarrini, S. et al. (2006) Chlorella virus MT325 encodes water and potassium channels that interact synergistically. Proceedings of the National Academy of Sciences of the United States of America 103, 5355–5360.
[9] Gazzarrini, S., Van Etten, J.L., DiFrancesco, D., Thiel, G. and Moroni, A. (2002) Voltage-dependence of virus-encoded miniature K^+ channel Kcv. Journal of Membrane Biology 187, 15–25.
[10] Hertel, B. et al. (2006) Elongation of outer transmembrane domain alters function of miniature K^+ channel Kcv. Journal of Membrane Biology 210, 21–29.
[11] Kang, M., Moroni, A., Gazzarrini, S. and Van Etten, J.L. (2003) Are chlorella viruses a rich source of ion channel genes? Febs Letters 552, 2–6.
[12] Gazzarrini, S. et al. (2004) Long distance interactions within the potassium channel pore are revealed by molecular diversity of viral proteins. Journal of Biological Chemistry 279, 28443–28449.
[13] Rosenberg, R.L. and East, J.E. (1992) Cell-free expression of functional shaker potassium channels. Nature 360, 166–169.
[14] Berrier, C. et al. (2004) Cell-free synthesis of a functional ion channel in the absence of a membrane and in the presence of detergent. Biochemistry 43, 12585–12591.
[15] Clayton, D. et al. (2004) Total chemical synthesis and electrophysiological characterization of mechanosensitive channels from *Escherichia coli* and *Mycobacterium tuberculosis*. Proceedings of the National Academy of Sciences of the United States of America 101, 4764–4769.
[16] Valiyaveetil, F.I., Sekedat, M., Muir, T.W. and MacKinnon, R. (2004) Semisynthesis of a functional K^+ channel. Angewandte Chemie-International Edition 43, 2504–2507.
[17] Lyford, L.K. and Rosenberg, R.L. (1999) Cell-free expression and functional reconstitution of homo-oligomeric alpha 7 nicotinic acetylcholine receptors into planar lipid bilayers. Journal of Biological Chemistry 274, 25675–25681.

[18] Hirsh, J.K. and Wu, C.H. (1997) Palytoxin-induced single channel currents from the sodium pump synthesized by in vitro expression. Toxicon 35, 169–176.
[19] Elbaz, Y., Steiner-Mordoch, S., Danieli, T. and Schuldiner, S. (2004) In vitro synthesis of fully functional EmrE, a multidrug transporter, and study of its oligomeric state. Proceedings of the National Academy of Sciences of the United States of America 101, 1519–1524.
[20] Braha, O. et al. (1997) Designed protein pores as components for biosensors. Chemistry and Biology 4, 497–505.
[21] Cheley, S., Braha, G., Lu, X.F., Conlan, S. and Bayley, H. (1999) A functional protein pore with a "retro" transmembrane domain. Protein Science 8, 1257–1267.
[22] Miles, G., Cheley, S., Braha, O. and Bayley, H. (2001) The staphylococcal leukocidin bicomponent toxin forms large ionic channels. Biochemistry 40, 8514–8522.
[23] Miles, G., Bayley, H. and Cheley, S. (2002) Properties of *Bacillus cereus* hemolysin II: a heptameric transmembrane pore. Protein Science 11, 1813–1824.
[24] Chanda, B., Asamoah, O.K., Blunck, R., Roux, B. and Bezanilla, F. (2005) Gating charge displacement in voltage-gated ion channels involves limited transmembrane movement. Nature 436, 852–856.
[25] Cordero-Morales, J.F. et al. (2006) Molecular determinants of gating at the potassium-channel selectivity filter. Nature Structural and Molecular Biology 13, 311–318.
[26] Doyle, D.A. et al. (1998) The structure of the potassium channel: molecular basis of K^+ conduction and selectivity. Science 280, 69–77.
[27] Jan, L.Y. and Jan, Y.N. (1997) Cloned potassium channels from eukaryotes and prokaryotes. Annual Review of Neuroscience 20, 91–123.
[28] LeMasurier, M., Heginbotham, L. and Miller, C. (2001) KcsA: it's a potassium channel. Journal of General Physiology 118, 303–313.
[29] Noskov, S.Y., Berneche, S. and Roux, B. (2004) Control of ion selectivity in potassium channels by electrostatic and dynamic properties of carbonyl ligands. Nature 431, 830–834.
[30] MacKinnon, R. (1991) Determination of the subunit stoichiometry of a voltage-activated potassium channel. Nature 350, 232–235.
[31] MacKinnon, R., Aldrich, R.W. and Lee, A.W. (1993) Functional stoichiometry of shaker potassium channel inactivation. Science 262, 757–759.
[32] Heginbotham, L., Odessey, E. and Miller, C. (1997) Tetrameric stoichiometry of a prokaryotic K^+ channel. Biochemistry 36, 10335–10342.
[33] Hoover, D.M. and Lubkowski, J. (2002) DNAWorks: an automated method for designing oligonucleotides for PCR-based gene synthesis. Nucleic Acids Research 30.
[34] Cheley, S., Xie, H. and Bayley, H. (2006) A genetically encoded pore for the stochastic detection of a protein kinase. ChemBioChem 7, 1923–1927.
[35] Don, R.H., Cox, P.T., Wainwright, B.J., Baker, K. and Mattick, J.S. (1991) Touchdown pcr to circumvent spurious priming during gene amplification. Nucleic Acids Research 19, 4008.
[36] Howorka, S., Cheley, S. and Bayley, H. (2001) Sequence-specific detection of individual DNA strands using engineered nanopores. Nature Biotechnology 19, 636–639.
[37] Howorka, S. and Bayley, H. (1998) Improved protocol for high-throughput cysteine scanning mutagenesis. Biotechniques 25, 764.
[38] Laemmli, U.K. (1970) Cleavage of structural proteins during the assembly of the head of bacteriophage T4. Nature 227, 680–685.
[39] Montal, M. and Mueller, P. (1972) Formation of bimolecular membranes from lipid monolayers and a study of their electrical properties. Proceedings of the National Academy of Sciences of the United States of America 69, 3561–3566.
[40] Lu, Q. and Miller, C. (1995) Silver as a probe of pore-forming residues in a potassium channel. Science 268, 304–307.
[41] Cooper, E., Couturier, S. and Ballivet, M. (1991) Pentameric structure and subunit stoichiometry of a neuronal nicotinic acetylcholine-receptor. Nature 350, 235–238.
[42] Miles, G., Movileanu, L. and Bayley, H. (2002) Subunit composition of a bicomponent toxin: staphylococcal leukocidin forms an octameric transmembrane pore. Protein Science 11, 894–902.
[43] Pagliuca, C. et al. (2007) Molecular properties of Kcv, a virus encoded K^+ channel. Biochemistry (accessed 01.06.07).
[44] Shim, J.W. and Gu, L.Q. (2007) Stochastic sensing on a modular chip containing a single ion channel. Analytical Chemistry (accessed 02.09.07).
[45] Bayley, H. (2004) Single-molecule non-covalent and covalent chemistry in a protein nanoreactor. Abstracts of Papers of the American Chemical Society 228, U301.
[46] Movileanu, L., Howorka, S., Braha, O. and Bayley, H. (2000) Detecting protein analytes that modulate transmembrane movement of a polymer chain within a single protein pore. Nature Biotechnology 18, 1091–1095.
[47] Jung, Y., Cheley, S., Braha, O. and Bayley, H. (2005) The internal cavity of the staphylococcal alpha-hemolysin pore accommodates similar to 175 exogenous amino acid residues. Biochemistry 44, 8919–8929.
[48] Braha, O. et al. (2000) Simultaneous stochastic sensing of divalent metal ions. Nature Biotechnology 18, 1005–1007.